Modeling of Composite Beams and Plates
for Static and Dynamic Analysis

P.27

Interim Semi-Annual Report
NASA Grant NAG-1-1094
17 January – 16 July 1992

Prof. Dewey H. Hodges, Principal Investigator
Dr. Vladislav G. Sutyrin, Post Doctoral Fellow
Bok Woo Lee, Graduate Research Assistant
School of Aerospace Engineering
Georgia Institute of Technology
Atlanta, Georgia 30332-0150

Summary of Progress Prior to This Period

The main purpose of this research has been to develop a rigorous theory and corresponding computational algorithms for through-the-thickness analysis of composite plates. This type of analysis is needed in order to find the elastic stiffness constants for a plate and to post-process the resulting plate solution in order to find approximate three-dimensional displacement, strain, and stress distributions throughout the plate.

We have settled on the variational-asymptotical method (VAM)[1] as a suitable framework in which to solve these types of problems. The VAM was applied to laminated plates with constant thickness in the work of Atılgan and Hodges[2]. The corresponding geometrically nonlinear global deformation analysis of plates was developed by Hodges, Atılgan, and Danielson[3]. A different application of VAM, along with numerical results, was obtained by Hodges, Lee, and Atılgan[4]. (Copies of these papers have been delivered to Mr. Hinnant.)

In Ref. 2, the "first approximation" is exactly the same as classical laminated plate theory. The "second approximation" takes transverse shear deformation into account and is developed only for plates with certain restrictions in their construction. To remove the restrictions one must "kill" certain interaction terms in the strain energy, and the means for doing so for general laminated plates were not given in that paper.

In Ref. 3, a set of kinematical and intrinsic equilibrium equations are derived for large deflection and rotation but with small strain. The relationship between the drilling rotation and the other kinematical variables gives new insight into the drilling moment and its role in beam-plate connectivity. This work has shown that drilling type rotation is not an independent degree of freedom in plate theory. An applied drilling moment at a point on a plate is not resisted at all by the plate. Such a moment, in order to have any physical resistance from the plate, must be applied over a finite area. Other than this, a point drilling moment can only be resisted by a plate if the plate model is derived from couple-stress elasticity[5].

The development in Ref. 4 includes transverse shear in the "first approximation" and is stopped there. Results from this theory were compared, for the cylindrical bending case, with results from the exact solution of Pagano[6] for cross-ply laminated plates. The resulting theory, termed a "neo-classical" theory, is at least as good as classical theory in every case and for some cases superior to it. Further work was judged to be needed in order to correlate with shear-coupled laminates, also treated by Pagano[7].

Summary of Work Done During This Period

Work during this reporting period has continued along two lines: (1) We have continued to evaluate the neo-classical plate theory (NCPT) for the shear-coupled laminates and (2) we began to explore, with permission from the technical monitor, what kinds of considerations would be involved to model plates with nonuniform thickness, which has led to considerable progress toward development of higher approximations of our constant thickness plate models.

Evaluation of NCPT for Shear-Coupled Laminates

Upon finishing the validation of NCPT for bidirectional plates, we continued to evaluate the response of plates with arbitrary stacking sequences. This is a rather challenging problem. Since the fiber orientations are not parallel to the axis of each laminate, the influence of shear-coupling becomes more evident for this type of laminated plates. When the fiber orientation coincides with the principal elastic axes of each laminate no shear-coupling terms exists. For validating the

theory, example cases are chosen from Pagano[7], in which the exact, closed-form three-dimensional solutions are available. The results shows that the new theory (NCPT) is more accurate than classical laminated plate theory (CPT) when thickness of plate increases. Since NCPT has more kinematical variables than CPT, we expect it to be more accurate for thick plates.

After summarizing the through-the-thickness analysis, we will present the governing equations for the global plate analysis with arbitarary stacking sequences. Finally, we will present the solutions.

Three-Dimensional Description Consider a plate of constant thickness h composed of layers, each of which is homogeneous and possesses monoclinic material symmetry about its mid-plane; a schematic of the plate mid-surface is shown in Fig. 1. Let us introduce Cartesian coordinates x_i so that x_α denotes lengths along orthogonal straight lines in the mid-surface of the undeformed plate, and $x_3 = h\zeta$ is the distance of an arbitrary point to the mid-surface in the undeformed plate, where $-\frac{1}{2} \leq \zeta \leq \frac{1}{2}$. Throughout the analysis, Greek indices assume values 1 or 2; Latin indices assume values 1, 2, and 3; and repeated indices are summed over their ranges.

Now, letting $\mathbf{b}_i$ denote an orthogonal reference triad along the undeformed plate coordinate lines, one can express the position vector from a fixed point O to an arbitrary point as

$$\hat{\mathbf{r}}(x_1, x_2, \zeta) = x_\alpha \mathbf{b}_\alpha + h\zeta \mathbf{b}_3 = \mathbf{r}(x_1, x_2) + h\zeta \mathbf{b}_3 \tag{1}$$

The position vector to the mid-surface is also the average position of points along the normal line, at a particular value of x_1 and x_2, so that

$$\mathbf{r} = \int_{-\frac{1}{2}}^{\frac{1}{2}} \hat{\mathbf{r}} d\zeta = \langle \hat{\mathbf{r}} \rangle \tag{2}$$

The angle brackets $\langle \rangle$ are used throughout the paper to denote the integral through the thickness.

Now, in accordance with Ref. 3 the position vector of any point in the deformed plate is

$$\hat{\mathbf{R}}(x_1, x_2, \zeta) = \mathbf{R}(x_1, x_2) + h\zeta \mathbf{B}_3(x_1, x_2) + h w_i(x_1, x_2, \zeta) \mathbf{B}_i(x_1, x_2) \tag{3}$$

where $\mathbf{R}$ is defined as

$$\mathbf{R}(x_1, x_2) = \langle \hat{\mathbf{R}}(x_1, x_2, \zeta) \rangle = \mathbf{r}(x_1, x_2) + \mathbf{u}(x_1, x_2) \tag{4}$$

and where $\mathbf{u}$ is the plate displacement vector, defined as the position vector from a point on the undeformed plate mid-surface to the corresponding point on the average surface of the deformed plate. The $\mathbf{B}_i$ triad is defined so that

$$\mathbf{B}_1 \cdot \mathbf{R}_{,2} = \mathbf{B}_2 \cdot \mathbf{R}_{,1} \tag{5}$$

and $\mathbf{B}_3 = \mathbf{B}_1 \times \mathbf{B}_2$ is parallel to $\langle \zeta \hat{\mathbf{R}} \rangle$. These definitions give rise to the same kinematical constraints on the warping as suggested by Hodges *et al.*[3]

$$\langle w_i \rangle = 0 \qquad \langle \zeta w_\alpha \rangle = 0 \tag{6}$$

3

We now turn to the strain field, details of which can be found in Ref. 2. First we arrange the six strain components into a matrix form so that

$$\Gamma = \lfloor \Gamma_e \quad 2\Gamma_s \quad \Gamma_t \rfloor^T \tag{7}$$

where Γ_e includes the extensional and in-plane shearing strains, and Γ_s and Γ_t contains the transverse shear and transverse normal strains, respectively. Thus,

$$\begin{aligned}
\Gamma_e &= \lfloor \Gamma_{11} \quad 2\Gamma_{12} \quad \Gamma_{22} \rfloor^T \\
2\Gamma_s &= \lfloor 2\Gamma_{13} \quad 2\Gamma_{23} \rfloor^T \\
\Gamma_t &= \Gamma_{33}
\end{aligned} \tag{8}$$

Next, for notational convenience, we introduce the matrix operators

$$\partial_t = h \begin{bmatrix} \frac{\partial}{\partial x_1} \\ \frac{\partial}{\partial x_2} \end{bmatrix} \qquad \partial_e = h \begin{bmatrix} \frac{\partial}{\partial x_1} & 0 \\ \frac{\partial}{\partial x_2} & \frac{\partial}{\partial x_1} \\ 0 & \frac{\partial}{\partial x_2} \end{bmatrix} \tag{9}$$

and generalized strain measures in matrix form given by

$$\begin{aligned}
\epsilon &= \lfloor \epsilon_{11} \quad 2\epsilon_{12} \quad \epsilon_{22} \rfloor^T \\
K &= \lfloor K_{11} \quad 2\kappa_{12} \quad K_{22} \rfloor^T \\
2\gamma &= \lfloor 2\gamma_{13} \quad 2\gamma_{23} \rfloor^T
\end{aligned} \tag{10}$$

where ϵ_{11} and ϵ_{22} are the plate extensional strain measures, $2\epsilon_{12}$ is the plate in-plane shear strain measure, $2\gamma_{\alpha 3}$ are the plate transverse shear strain measures, K_{11} and K_{22} are the plate bending measures, and $2\kappa_{12} = K_{12} + K_{21}$ is the plate twisting measure. All these measures are functions only of x_1 and x_2, and their explicit forms for large deformation are given in Ref. 3.

Denoting the in-plane warping by

$$w_\| = \lfloor w_1 \quad w_2 \rfloor^T \tag{11}$$

one can now write the Jaumann strain components following Ref. 3 as

$$\begin{aligned}
\Gamma_e &= \epsilon + \zeta K h + \partial_e w_\| \\
2\Gamma_s &= w_\|' + 2\gamma + \partial_t w_3 \\
\Gamma_t &= w_3'
\end{aligned} \tag{12}$$

where $(\ )'$ denotes the derivative with respect to ζ.

A similar procedure can be followed for the conjugate stresses so that

$$\begin{aligned}
Z_e &= \lfloor Z_{11} \quad Z_{12} \quad Z_{22} \rfloor^T \\
Z_s &= \lfloor Z_{13} \quad Z_{23} \rfloor^T \\
Z_t &= Z_{33}
\end{aligned} \tag{13}$$

4

where Z_e contains the extensional and in-plane shear stresses while Z_s and Z_t have the transverse shear and transverse normal stresses. The stress components may then be written in a matrix form as

$$Z = \lfloor Z_e \quad Z_s \quad Z_t \rfloor^T \tag{14}$$

In light of this, the three-dimensional constitutive law can be expressed as

$$\begin{Bmatrix} Z_e \\ Z_s \\ Z_t \end{Bmatrix} = \begin{bmatrix} D_e & D_{es} & D_{et} \\ D_{es}^T & D_s & D_{st} \\ D_{et}^T & D_{st}^T & D_t \end{bmatrix} \begin{Bmatrix} \Gamma_e \\ 2\Gamma_s \\ \Gamma_t \end{Bmatrix} \tag{15}$$

where D_e, D_{es}, D_{et}, D_s, D_{st}, and D_t are 3×3, 3×2, 3×1, 2×2, 2×1, and 1×1 matrices, respectively. Here, this law is written for directions parallel to plate coordinate axes, which are not in general along the material axis. Therefore, the material constants, D's, are the transformed values from material axis to the plate axis.

The plate strain energy per unit area can then be written as

$$J = \frac{1}{2} \left\langle Z^T \Gamma \right\rangle \tag{16}$$

Following Ref. 2, we decompose the strain energy into two positive definite, quadratic forms. Here we define the extensional strain energy $J_\parallel$, and the transverse strain energy $J_\perp$ (containing contributions from both transverse normal and shear strains) as

$$\begin{aligned} J_\parallel &= \min_{\Gamma_s, \Gamma_t} J \\ J_\perp &= J - J_\parallel \end{aligned} \tag{17}$$

When the material fiber direction is oriented parallel to the plane of the plate, such that each lamina exhibits a monoclinic symmetry, D_{es} and D_{st} will vanish. In this case the extensional and transverse energies can be written in terms of the three-dimensional material properties in the following simple form

$$\begin{aligned} 2J_\parallel &= \langle \Gamma_e^T D_\parallel \Gamma_e \rangle \\ 2J_\perp &= \langle 2\Gamma_s^T D_s 2\Gamma_s + D_t \left(\Gamma_t + D_\perp \Gamma_e \right)^2 \rangle \end{aligned} \tag{18}$$

where

$$D_\parallel = D_e - D_{et} D_\perp \qquad D_\perp = D_t^{-1} D_{et}^T \tag{19}$$

This completes the three-dimensional description of the displacement, strain, and stress fields. These three-dimensional fields are not really suitable for plate analysis because of the three-dimensional warping variables w_i. We now turn to elimination of the warping by dimensional reduction.

Dimensional Reduction In the following sections, we will apply the variational-asymptotical method of Ref. 1 for nonhomogeneous, laminated plates in pursuit of a first approximation of the plate strain energy. Before doing so, however, it is appropriate to discuss the estimation procedure. First, we introduce upper bounds on the in-plane, bending, and transverse shear strain measures ε_e, ε_b, and ε_s, respectively, such that

$$\sqrt{\epsilon^T \epsilon} \leq \varepsilon_e \qquad \frac{h}{2} \sqrt{K^T K} \leq \varepsilon_b \qquad \sqrt{2\gamma^T 2\gamma} \leq \varepsilon_s \tag{20}$$

5

For the first approximation we need only to keep terms in the strain field that are of the order of ε where

$$\varepsilon_e + \varepsilon_b + \varepsilon_s \leq \varepsilon \tag{21}$$

This implies that we will have strain energy density of the order $\mu\varepsilon^2$ where μ is of the order of the elastic moduli.

In order to take advantage of the physical aspects of plate deformation, we introduce another small parameter h/ℓ, where ℓ is the smallest constant for which all of the following hold for all possible combinations of α and β

$$\sqrt{\epsilon_{,\alpha}^T \epsilon_{,\beta}} \leq \frac{\varepsilon_e}{\ell} \quad \frac{h}{2}\sqrt{K_{,\alpha}^T K_{,\beta}} \leq \frac{\varepsilon_b}{\ell} \quad \sqrt{2\gamma_{,\alpha}^T 2\gamma_{,\beta}} \leq \frac{\varepsilon_s}{\ell} \tag{22}$$

One may think of ℓ as the wavelength of the deformation pattern.

Rather than write out complete expressions for the strain field, we will only write the terms needed for the first approximation. By consideration of the above set of estimation parameters, the strain expression can be approximated as

$$\begin{aligned}
\Gamma_e &= \epsilon + \zeta Kh \\
2\Gamma_s &= 2\gamma + w_{\parallel}' \\
\Gamma_t &= w_3'
\end{aligned} \tag{23}$$

Thus, the warping is not present in extensional energy, and the only part of the strain energy remaining to be minimized is the transverse energy

$$\begin{aligned}
2J_{\perp} &= \left\langle D_t \left[w_3' + D_{\perp}(\epsilon + \zeta Kh) \right]^2 \right\rangle \\
&+ \left\langle (2\gamma + w_{\parallel}')^T D_s (2\gamma + w_{\parallel}') \right\rangle
\end{aligned} \tag{24}$$

The variational-asymptotical method calls for the minimization of this strain energy expression with respect to the warping, with the constraints given in Eq. (6), resulting in

$$\begin{aligned}
w_3 &= D_{\perp 1}\epsilon + D_{\perp 2}Kh \\
w_{\parallel} &= \left[\frac{1}{12}(H_{s1} - 8H_{s2})(\langle \zeta H_{s1} \rangle - 8\langle \zeta H_{s2} \rangle)^{-1} - I_2\zeta \right] 2\gamma
\end{aligned} \tag{25}$$

in which I_2 is the 2×2 identity matrix and

$$\begin{aligned}
D_{\perp 1}' &= -D_{\perp} & D_{\perp 2}' &= -\zeta D_{\perp} \\
H_{s1}' &= D_s^{-1} & H_{s2}' &= \frac{\zeta^2}{2} D_s^{-1}
\end{aligned} \tag{26}$$

These expressions for the warping are determined uniquely by imposing the continuity of $D_{\perp\alpha}$ and $H_{s\alpha}$ between the layers together with constraints Eq. (6) so that

$$\langle D_{\perp\alpha} \rangle = \langle H_{s\alpha} \rangle = 0 \tag{27}$$

6

for out-of-plane and in-plane warping, respectively. These constraints guarantee that warping functions are continuous. However, strain and stress, which are functions of the derivatives of the warping, may or may not be continuous.

The strain energy per unit area of the plate is obtained by substituting the warping from Eq. (25) into the strain energy, yielding

$$J = \frac{1}{2} \left[\epsilon^T \left(A\epsilon + 2BK \right) + K^T DK + 2\gamma^T G 2\gamma \right] \tag{28}$$

where

$$\begin{aligned} A &= h\langle D_\parallel \rangle & B &= h^2 \langle \zeta D_\parallel \rangle \\ D &= h^3 \langle \zeta^2 D_\parallel \rangle & G &= h\langle g^T D_s \, g \rangle \end{aligned} \tag{29}$$

and where

$$g = \frac{1}{12} \left(1 - 4\zeta^2 \right) D_s^{-1} (\langle \zeta H_{s1} \rangle - 8\langle \zeta H_{s2} \rangle)^{-1} \tag{30}$$

Note that $D_\parallel$ corresponds to $\overline{Q}$, the well known transformed reduced stiffness matrix from classical laminated plate theory[8]. It is possible to define the force, moment and transverse shear stress resultants N, M, and Q respectively, as

$$\begin{aligned} N &= h\langle Z_e \rangle = \left(\frac{\partial J}{\partial \epsilon} \right)^T \\ M &= h^2 \langle \zeta Z_e \rangle = \left(\frac{\partial J}{\partial K} \right)^T \\ Q &= h\langle Z_s \rangle = \left[\frac{\partial J}{\partial (2\gamma)} \right]^T \end{aligned} \tag{31}$$

Then, based on the strain energy, the plate constitutive law can be expressed as

$$\begin{Bmatrix} N \\ M \\ Q \end{Bmatrix} = \begin{bmatrix} A & B & 0 \\ B^T & D & 0 \\ 0 & 0 & G \end{bmatrix} \begin{Bmatrix} \epsilon \\ K \\ 2\gamma \end{Bmatrix} \tag{32}$$

Note that transverse normal stress is zero in this theory, and thus, we should not expect the transverse normal strain to be very accurate from Eqs. (12) unless we extend the theory to higher approximations. Similarly, we do not expect the transverse shear stress and strain to be very accurate with the present theory, since some important contributions to its detailed variation are associated with h/ℓ corrections to the energy[1]. These quantities can be obtained from integrating the three-dimensional equilibrium equations through the thickness to get the transverse shear and normal stresses and applying the three-dimensional constitutive law to get the transverse shear and normal strains.

This concludes the dimensional reduction. The global deformation equations[3], along with these plate constitutive equations, comprise what we term the neo-classical theory. (Note that the displacement shift mentioned in Refs. 2 and 3 is not necessary with this theory, and thus $2\gamma^* = 2\gamma$.) With the warping known in terms of ϵ, K, and 2γ, which in turn are known through solution of the global deformation problem, it is now possible to evaluate three-dimensional approximations of

displacement, strain, and stress fields. For the purpose of validating the stiffness model and field relations, however, only a specialized version of the global deformation analysis is undertaken here.

Linear Plate Equations The global deformation equations that correspond to the above strain energy function were developed in Ref. 3. Since ϵ, K, and 2γ are nonlinear functions of the displacement and rotation variables, this theory is applicable to large deformation of plates, and these can now be obtained by solving a specific problem. Here, rather than repeat the entire formulation, we will specialize it for linear, cylindrical bending problems, which we will use below for validation of the dimensional reduction scheme of the previous section.

Kinematical equations from Ref. 3 for the linear case are given as

$$
\begin{aligned}
\epsilon_{11} &= u_{1,1} \\
2\epsilon_{12} &= u_{1,2} + u_{2,1} \\
\epsilon_{22} &= u_{2,2} \\
K_{11} &= \theta_{1,1} \\
2\kappa_{12} &= \theta_{1,2} + \theta_{2,1} \\
K_{22} &= \theta_{2,2} \\
2\gamma_{13} &= \theta_1 + u_{3,1} \\
2\gamma_{23} &= \theta_2 + u_{3,2}
\end{aligned}
\tag{33}
$$

where $u_i = \mathbf{u} \cdot \mathbf{b}_i$ and $\theta_\alpha = \mathbf{B}_3 \cdot \mathbf{b}_\alpha$.

Similarly, equilibrium equations are

$$
\begin{aligned}
N_{11,1} + N_{12,2} + f_1 &= 0 \\
N_{12,1} + N_{22,2} + f_2 &= 0 \\
Q_{1,1} + Q_{2,2} + f_3 &= 0 \\
M_{11,1} + M_{12,2} - Q_1 &= 0 \\
M_{12,1} + M_{22,2} - Q_2 &= 0
\end{aligned}
\tag{34}
$$

where f_i are the applied loads per unit area of the plate.

Cylindrical Bending Analysis Consider a plate of length L along x_1 and infinite width in the x_2 direction shown in Fig. 2. All derivatives with respect to x_2 are zero which causes many of the variables in the above equilibrium, constitutive, and kinematical equations to drop out.

In the case of cylindrical bending, the plate is subject to sinusoidal surface loading of the form

$$
f_3(x_1) = p_0 \sin(px_1)
\tag{35}
$$

where $p = \frac{\pi}{L}$ and $f_\alpha = 0$. For the three-dimensional analysis, we assume the loading f_3 to be imposed in the form of an upper surface traction.

We consider a simply supported plate, the boundary conditions of which are

$$
u_3(0) = u_3(L) = 0 \qquad u_{\alpha,1}(0) = u_{\alpha,1}(L) = 0 \qquad \theta_{\alpha,1}(0) = \theta_{\alpha,1}(L) = 0
\tag{36}
$$

8

The governing system of equations can be put into a matrix form by defining generalized coordinates, strain measures, stress and moment results, and loading. Let

$$q = \lfloor u_1 \quad u_2 \quad \theta_1 \quad \theta_2 \quad u_3 \rfloor^T \tag{37}$$

$$\varepsilon = \lfloor \epsilon_{11} \quad 2\epsilon_{12} \quad \kappa_{11} \quad 2\kappa_{12} \quad 2\gamma_{13} \quad 2\gamma_{23} \rfloor^T \tag{38}$$

$$F = \lfloor N_{11} \quad N_{12} \quad M_{11} \quad M_{12} \quad Q_1 \quad Q_2 \rfloor^T \tag{39}$$

$$f = \lfloor 0 \quad 0 \quad 0 \quad 0 \quad -f_3 \rfloor^T \tag{40}$$

Eqs. (33) can be written as

$$\varepsilon = \mathcal{D} \, q \tag{41}$$

where

$$\mathcal{D} = \begin{bmatrix} \partial & 0 & 0 & 0 & 0 \\ 0 & \partial & 0 & 0 & 0 \\ 0 & 0 & \partial & 0 & 0 \\ 0 & 0 & 0 & \partial & 0 \\ 0 & 0 & 1 & 0 & \partial \\ 0 & 0 & 0 & 1 & 0 \end{bmatrix} = \begin{bmatrix} \partial & 0 & 0 & 0 & 0 \\ 0 & \partial & 0 & 0 & 0 \\ 0 & 0 & \partial & 0 & 0 \\ 0 & 0 & 0 & \partial & 0 \\ 0 & 0 & 0 & 0 & \partial \\ 0 & 0 & 0 & 0 & 0 \end{bmatrix} + \begin{bmatrix} 0 & 0 & 0 & 0 & 0 \\ 0 & 0 & 0 & 0 & 0 \\ 0 & 0 & 0 & 0 & 0 \\ 0 & 0 & 0 & 0 & 0 \\ 0 & 0 & 1 & 0 & 0 \\ 0 & 0 & 0 & 1 & 0 \end{bmatrix} = \partial^* + k \tag{42}$$

in which ∂ denotes the derivative with respect to x_1. Eqs. (34) can be written as

$$f = \mathcal{E} \, F \tag{43}$$

where

$$\mathcal{E} = \begin{bmatrix} \partial & 0 & 0 & 0 & 0 & 0 \\ 0 & \partial & 0 & 0 & 0 & 0 \\ 0 & 0 & \partial & 0 & -1 & 0 \\ 0 & 0 & 0 & \partial & 0 & -1 \\ 0 & 0 & 1 & 0 & \partial & 0 \end{bmatrix} = \partial^{*T} - k^T \tag{44}$$

Now plate constitutive equation can be written as

$$F = K^* \varepsilon \tag{45}$$

where

$$K^* = \begin{bmatrix} A^* & B^* & 0 \\ B^* & D^* & 0 \\ 0 & 0 & G \end{bmatrix} \tag{46}$$

Here the starred matrices are 2×2 sub-matrices consisting of the first 2 rows and columns of the corresponding matrices in Eqs. (32), resulting in K^* being a 6×6 matrix. So the given problem

yields 17 equations in terms of 17 unknowns. Combining Eqs. (41), (43), and (45), the equilibrium equations can be written as

$$\left(\partial^{*T} - k^T\right) K^* \left(\partial^* + k\right) = f \tag{47}$$

which can be put into the form

$$M_c \, \ddot{q}_{,11} + C_c \, q_{,1} - K_c \, q = f \tag{48}$$

where

$$M_c = \begin{bmatrix} A_{11}^* & A_{12}^* & B_{11}^* & B_{12}^* & 0 \\ A_{12}^* & A_{22}^* & B_{12}^* & B_{22}^* & 0 \\ B_{11}^* & B_{12}^* & D_{11}^* & D_{12}^* & 0 \\ B_{12}^* & B_{22}^* & D_{12}^* & D_{22}^* & 0 \\ 0 & 0 & 0 & 0 & G_{11} \end{bmatrix} = \begin{bmatrix} A^* & B^* & 0 \\ B^* & D^* & 0 \\ 0 & 0 & G_{11} \end{bmatrix} \tag{49}$$

$$C_c = \begin{bmatrix} 0 & 0 & 0 & 0 & 0 \\ 0 & 0 & 0 & 0 & 0 \\ 0 & 0 & 0 & 0 & -G_{11} \\ 0 & 0 & 0 & 0 & -G_{12} \\ 0 & 0 & G_{11} & G_{12} & 0 \end{bmatrix} \tag{50}$$

$$K_c = \begin{bmatrix} 0 & 0 & 0 & 0 & 0 \\ 0 & 0 & 0 & 0 & 0 \\ 0 & 0 & G_{11} & G_{12} & 0 \\ 0 & 0 & G_{12} & G_{22} & 0 \\ 0 & 0 & 0 & 0 & 0 \end{bmatrix} = \begin{bmatrix} 0 & 0 & 0 \\ 0 & G & 0 \\ 0 & 0 & 0 \end{bmatrix} \tag{51}$$

The above equation can be solved directly with associated boundary conditions. But let us take advantage of the sparcity of matrices in the equation. We can break down this equation as follows

$$A^* \, u_{,11} + B^* \, \theta_{,11} = 0 \tag{52}$$

$$B^* \, u_{,11} + D^* \, \theta_{,11} - \lfloor G_{11} \quad G_{12} \rfloor^T u_{3,1} - G \, \theta = 0 \tag{53}$$

$$G_{11} \, u_{3,11} + \lfloor G_{11} \quad G_{12} \rfloor \, \theta = -f_3 \tag{54}$$

when u and θ are arranged as

$$u = \lfloor u_1 \quad u_2 \rfloor^T \qquad \theta = \lfloor \theta_1 \quad \theta_2 \rfloor^T \tag{55}$$

Since f_3 is a simple sinusoidal function given in Eq. (35), θ can be uncoupled by putting Eqs. (52) and (54) into Eq. (53) yielding

$$M_c^* \, \theta_{,11} + K_c^* \, \theta = f_c^* \, \frac{p_0}{p} \cos(px_1) \tag{56}$$

where

$$M_c^* = D^* - B^* A^{*-1} B^* \qquad K_c^* = \begin{bmatrix} 0 & 0 \\ 0 & \frac{G_{12}^2}{G_{11}} - G_{22} \end{bmatrix} \qquad f_c^* = \lfloor 1 \quad \frac{G_{12}}{G_{11}} \rfloor^T$$

10

Since M_c^* is symmetric, positive definite and K_c^* symmetric, Eq. (56) can be decoupled as is. Note that when plate is symmetrically layered up B^* matrix vanishes, resulting $M_c^* = D^*$.

Now, introducing the coordinate transformation

$$\theta = \phi\, y \qquad (57)$$

where ϕ is a eigenvector matrix, we diagonalize Eq. (56) which gives

$$M_d\, y_{,11} + K_d\, y = f_d\, \frac{p_0}{p} \cos(px_1) \qquad (58)$$

where

$$M_d = \phi^T M_c^* \phi \qquad K_d = \phi^T K_c^* \phi \qquad f_d = \phi^T f_c^* \qquad (59)$$

By solving above decoupled equations for y, we can recover original solution θ using Eq. (57). It is easy to shown that all integration constants produced in the calculation vanish for cylindrical bending. In other words, we need only to obtain particular solution for Eq. (56) or Eq. (58). Note that since effects of boundary layer belong to higher order for this type of first approximation, we can neglect a homogeneneous solution in the first place.

After some calculation, θ can be found. Also u_3 and u are determined by putting θ into Eqs. (52) and Eqs. (54). Rotations, in-plane displacements, and out-of-palne displacement are obtained as follows

$$\theta = \phi\, \left[K_d - p^2 M_d\right]^{-1} f_d\, \frac{p_0}{p} \cos(px_1) \qquad (60)$$

$$u = -A^{*-1} B^* \left[K_d - p^2 M_d\right]^{-1} f_d\, \frac{p_0}{p} \cos(px_1) \qquad (61)$$

$$u_3 = \frac{1}{G_{11}} \left(1 - \lfloor G_{11} \quad G_{12} \rfloor\, \phi\, \left[K_d - p^2 M_d\right]^{-1} f_d\right) \frac{p_0}{p^2} \sin(px_1) \qquad (62)$$

To recover three-dimensional fields, one can substitute values obtained for ϵ, K, and 2γ by taking derivatives of above expressions into Eqs. (25), (23), and (15), to get warping, strain, and stress, respectively. Note that all the strain measures can be calculated to order ε by using Eq. (23); however, Γ_e can be determined to order $h\varepsilon/\ell$ by use of Eq. (12). To avoid inconsistency, one should use Eq. (23) for all strain components when calculating the stress components. However, NCPT is more accurate than CPT since it picked up the general strain measures which do not appear in CPT. In other words, the extra strain measures reflect the effects of transverse shear deformatiom, resulting in a better solution:

For the purpose of comparing the displacement field with that of linear, three-dimensional elasticity, we need to determine the $\mathbf{b}_i$ measure numbers of the displacement field

$$z_i = \mathbf{b}_i \cdot \left(\hat{\mathbf{R}} - \hat{\mathbf{r}}\right) \qquad (63)$$

With the warping known from Eqs. (25) in terms of ϵ, K, and 2γ, and the triad $\mathbf{B}_i$ given as

$$\mathbf{B}_1 = \mathbf{b}_1 + \frac{u_{2,1}}{2}\mathbf{b}_2 - \theta_1 \mathbf{b}_3$$

$$\mathbf{B}_2 = -\frac{u_{2,1}}{2}\mathbf{b}_1 + \mathbf{b}_2 - \theta_2 \mathbf{b}_3 \qquad (64)$$

$$\mathbf{B}_3 = \theta_1 \mathbf{b}_1 - \theta_2 \mathbf{b}_2 + \mathbf{b}_3$$

11

The functions z_i can now be expressed in terms of global deformation variables. The result is that

$$z_1 = u_1 + h\zeta\theta_1 + hw_1$$
$$z_2 = u_2 - h\zeta\theta_2 + hw_2 \tag{65}$$
$$z_3 = u_3 + hw_3$$

where u_i, θ_α are obtainable in Eqs. (60), (61), and (62), and w_i in Eq. (25).

Results The intent of this section is to compare results from the exact solution with results from the present theory. The exact three-dimensional elasticity solution for cylindrical bending of angle ply laminated plates was obtained by Pagano[7], and the results presented herein labelled as "exact" generated from his equations. The material properties are[7]

$$E_L = 25 \times 10^6 \text{psi} \qquad E_T = 10^6 \text{psi}$$
$$G_{LT} = 0.5 \times 10^6 \text{psi} \qquad G_{TT} = 0.2 \times 10^6 \text{psi} \tag{66}$$
$$\nu_{LT} = \nu_{TT} = 0.25$$

where L signifies the direction parallel to the fibers and T the transverse direction. We evaluated all quantities obtainable from the neo-classical theory for this problem and compared those results with the exact solution for various values of L/h. We have chosen to present most of our results for L/h values of 10 and 4, which represent relativatively thin and thick plates, respectively.

For plotting the displacement, strain, and stress distributions the following normalized parameters are used

$$\overline{z}_\alpha = \frac{E_T h^2 z_\alpha(x_1,\zeta)}{L^3 p_0} \qquad \overline{z}_3 = \frac{100 E_T h^3 z_3(x_1,\zeta)}{L^4 p_0}$$
$$\overline{Z}_{\alpha\beta} = \frac{h^2 Z_{\alpha\beta}(x_1,\zeta)}{L^2 p_0} \qquad \overline{Z}_{\alpha 3} = \frac{h Z_{\alpha 3}(x_1,\zeta)}{L p_0} \tag{67}$$
$$\overline{\Gamma}_{ij} = \frac{E_L h^2 \Gamma_{ij}(x_1,\zeta)}{L^2 p_0}$$

The through-the-thickness distributions of in-plane displacement, transverse shear stress and strain are evaluated at $x_1 = 0$; while the distributions of out-of-plane displacement, in-plane stress and strain, transverse normal stress and strain are evaluated at $x_1 = L/2$. In all the results below, solid lines represent the exact solution, while dashed lines represent the present neo-classical plate theory (NCPT) results. Results from classical laminated plate theory (CPT), when distinct from NCPT results, are shown with long and short dashes.

The distributions of normalized displacements, strains, and stresses are obtained for the following three plates, in which each layer has the same thickness:

$$[15°]$$
$$[15°/ - 15°]$$
$$[30°/ - 30°]_{sym}$$

Results for these plates are presented in Figs. 3 – 19. Figs. 3 – 5 show the transverse displacement for these three configurations, respectively. Note the very close agreement between NCPT and the exact solution. NCPT is just slightly more flexible than the exact solution; it provides significant improvement over CPT as L/h becomes small, until L/h of approximately 10.

12

Figs. 6 and 7 show normalized out-of-plane displacement (z_3), in-plane displacement (z_1), in-plane strain (Γ_{11}) and shear strain ($2\Gamma_{12}$) for [15°] plate from top to bottom in the figures; Figs. 10 and 11 show the same quantities for [15°/ − 15°] plate. Figs. 8 and 9 show normalized in-plane stress (Z_{11}), transverse shear stress (Z_{13}) and strain ($2\Gamma_{13}$), transverse normal strain (Γ_{33}) for [15°] plate; Figs. 12 and 13 show the same quantities for [15°/ − 15°] plate.

Figs. 14 − 19 show the results for [30°/ − 30°]$_{sym}$ plate. Figs. 14 and 15 show normalized out-of-plane displacement (z_3), in-plane displacements (z_1, z_2), in-plane strain (Γ_{11}). Figs. 16 and 17 show normalized in-plane shear strain ($2\Gamma_{12}$), in-plane stress (Z_{11}) and shear stress (Z_{12}), and transverse shear stress (Z_{13}). Figs. 18 and 19 show normalized transverse shear stress (Z_{23}) and strain ($2\Gamma_{23}$), transverse normal stress (Z_{33}) and strain (Γ_{33}).

Transverse in-plane stresses (Z_{22}) are not shown since these have the same pattern as the corresponding in-plane stresses (Z_{11}). Note that transverse shear stresses in the figures are obtained from integrating the equilibrium equations of elasticity. Also note that transverse in-plane displacement (z_2), in-plane shear strain and stress ($2\Gamma_{12}$, Z_{12}) and transverse shear strain and stress ($2\Gamma_{23}$, Z_{23}) will differ from those of Pagano[7]. This stems from the different sign convention used for plotting in this work, resulting in the same magnitude but with opposite sign. Some of these quantities are also reported in graphical form in Ref. 9.

The in-plane displacements and strains from NCPT shown in Figs. 6, 7, 10, 11, 14 and 15 are much closer to the exact solution than those from CPT. One reason the in-plane strain and shear strain are so accurate is that Γ_e is calculated to $O(h\varepsilon/\ell)$ using Eq. (12). The in-plane stress and shear stress are essentially identical to that of CPT shown in Figs. 8, 9, 12, and 13 for the 1- and 2-layer cases. On the other hand, NCPT is better than CPT shown in Figs. 16 and 17 for the 4-layer case. This is because that NCPT has more kinematical varivables than CPT. Even though the difference is invisible for 1- and 2-layer cases, twisting curvature, which is a one of generalized strain measures used in NCPT, plays an important role for this specific example.

It is interesting to note that in Fig. 19, transverse shear stress (Z_{23}) from NCPT has sign changes around at the middle surface, while results from the exact solution are positive. Based on results obtained to date, we believe that an extension of the theory of Ref. 3 to a higher approximation still needs to be developed in order to improve the correlation of this and other three-dimensional field variables with the exact solution. However, interaction terms are present in the energy when a higher approximation is attempted, similar to those of Ref. 2; these must be killed, but the means for doing so were unknown until recently. This means was discovered in conjunction with the analysis of nonuniform thickness plates.

Higher Approximations and Plates with Nonuniform Thickness

During the last two months, we have been attempting to extend our methodology to deal with plates, the thickness of which varies spatially over the plate domain so that $h = h(x_1, x_2)$. In the process of doing this for isotropic plates, an additional degree of freedom for the normal line element was introduced on physical grounds, within the context of VAM. This degree of freedom involves the contraction of the normal line element. Although the contraction was not zero in the original theories, it was a "reactive" quantity. That is, it does not appear in the strain energy function explicitly, and it can be calculated in terms of other degrees of freedom of the normal line element. When the thickness is allowed to vary spatially over the plate, this degree of freedom appears explicitly in the reduced, two-dimensional strain energy function and must be regarded as an independent quantity. This new degree of freedom improved the correlation with three-dimensional results relative to classical theory, but the accuracy was still judged inadequate. Indeed, it was not

possible to show that the additional warping was of a higher order than this degree of freedom. Moreover, the motivation for introducing this degree of freedom was not at all systematic.

Dr. Sutyrin then discovered a powerful principle for identifying valid degrees of freedom in the dimensional reduction process. (This principle applies for development of beam, plate, and shell theories.) There exists an eigenvalue problem, the eigenvectors of which are the valid degrees of freedom for the structural member. They are valid in the sense that (1) they satisfy the appropriate interfacial conditions; (2) they guarantee that the above-mentioned interaction terms vanish; (3) they guarantee that any additional warping is of a higher order. They are not simple polynomials, in general. The degrees of freedom in classical theory, it turns out, are the eigenvectors associated with the zero eigenvalues for this eigenproblem. Sutyrin's eigen-principle should allow us to extend the earlier laminated plate theories to higher approximations in a rational manner.

If plates of constant thickness must be joined to plates of varying thickness, then both models must contain the same degrees of freedom. This means that the constant thickness model must be taken to a higher-order approximation so as to bring the same, or at least analogous degrees of freedom into the strain energies of both plates. The mathematics associated with this operation are quite difficult, involving functional analysis as well as the construction of non-trivial transformations to rid the strain energy of unneeded degrees of freedom. Unanswered questions also remain concerning the role of edge-zone behavior and penetration of the influence of self-equilibrated tractions on the plate edges.

To illustrate this, let us write the Jaumann strain components as

$$\Gamma_e = \epsilon + \zeta K h + \partial_e w_{\parallel}$$

$$2\Gamma_s = w'_{\parallel} + \partial_t w_3 \tag{68}$$

$$\Gamma_t = w'_3$$

The resulting warping will be different from the result of Eqs. (25), because 2γ has been set to equal to zero and its effect absorbed into w. It turns out that the warping variable can be written as

$$w_i(x_1, x_2, \zeta) = \sum_k q_k(x_1, x_2)\psi_{i_k}(\zeta) + v_i(x_1, x_2, \zeta) \tag{69}$$

where v_i represents additional warping and q_i the degrees of freedom associated with the ψ functions. The ψ's can be identified by means of the VAM procedure and Sutyrin's eigen-principle. The resulting two-dimensional strain energy function will contain the q functions and their derivatives. The process of identifying these "degrees of freedom" for the plate, as presented in the literature, is not straightforward. We have made some important progress recently in this identification procedure.

We consider a homogeneous, isotropic plate with thickness depending on only one in-plane coordinate and undergoing a stretching load; see Fig. 20. In order to solve this problem we have to introduce new degrees of freedom. It is clear that the average bending of the plate and rotating of normal line element are equal to zero here. Nevertheless there is a non-trivial deformation of normal line elements, which can be observed in the elasticity solution (which we approximated by a finite element solution). This deformation is shown schematically in Fig. 21. There is no known systematic way to introduce such deformations into classical theory or into Reissner's theory, which takes into account only the transverse shear deformation.

In order to introduce some new degrees of freedom in our analysis, we take the warping to be of the form of Eq. (69) where ψ is the shape function of a degree of freedom and q is the new degree

14

of freedom itself. The VAM procedure points to the best choice of the shape function ψ as an eigenvector of a natural eigenvalue problem for normal line element (a one-dimensional problem).

For example, the two degrees of freedom corresponding to the smallest nonzero eigenvalues can be represented as

$$w_\alpha = g_\alpha(x_1, x_2)\cos(2\pi\zeta) + v_\alpha \qquad (70)$$

and

$$w_3 = e(x_1, x_2)\sin(\pi\zeta) + v_3 \qquad (71)$$

for the homogeneous isotropic case. The degree of freedom g_1 (g for short) is responsible for in-plane deformation such as shown in Fig. 21, while the degree of freedom e describes contraction of the normal line element. The variable v models any *additional* warping, which is of a higher order and may be ignored in this example.

Fig. 22 shows comparison between g and e obtained from a 3-D solution (dashed line) and g and e from our new theory (solid line).

This approach has a natural generalization for dynamics problems. The above eigenvalues become eigenfrequencies in that context. Also, it is not difficult to obtain a suitable dynamical equation for each degree of freedom. In general, one would need to apply the theory to a wide class of problems and loading conditions in order to understand the appropriate number of degrees of freedom to be retained.

We expect to develop the dimensional reduction with the extensive use of computerized symbolic manipulation and the expertise of Dr. Sutyrin. As a fallback position, should a symbolic dimensional reduction not be possible, we can solve the minimization problems via one-dimensional finite elements (through-the-thickness). Both means are quite efficient for laminated plate problems. The through-the-thickness analysis is only done once for a given lay-up. The results for the elastic constants are used as input to the plate (two-dimensional) analysis, and the influence functions are used to recover approximations for the three-dimensional field variables once the two-dimensional problem is solved.

Future Work

In the balance of the grant we intend to apply Sutyrin's eigen-principle to develop a refined theory for laminated plates of constant thickness. If there is time we will make this theory capable of modeling the most general type of nonhomogeneous, anisotropic plate, subject only to the restrictions that the strain is small and that neither geometry nor properties vary with x_1 and x_2. Development of an interior global deformation analysis for constant thickness anisotropic plates would then be possible, but it appears that this should be addressed only after the degrees of freedom for a general analysis are identified. This means that the boundary energy and nonuniform thickness problems should be addressed first. We are seeking to obtain funding from NASA to carry this out.

References

1. Berdichevsky, Victor L., "Variational-Asymptotic Method of Constructing a Theory of Shells," *PMM*, Vol. 43, No. 4, 1979, pp. 664 – 687.

2. Atilgan, A. R., and Hodges, D. H.,"On the Strain Energy of Laminated Composite Plates," *International Journal of Solids and Structures*, 1992, to appear.

3. Hodges, D. H., Atılgan, A. R., and Danielson, D. A., "A Geometrically Nonlinear Theory of Elastic Plates," AIAA Paper 92-2281. *Proceedings of the 33rd Structures, Structural Dynamics, and Materials Conference*, Dallas, Texas, April 13 – 15, 1992, pp. 878 – 889, *Journal of Applied Mechanics*, to appear.

4. Hodges, D. H., Lee, B. W., and Atılgan, A. R., "Application of the Variational-Asymptotical Method to Laminated Composite Plates," AIAA Paper 92-2357, *Proceedings of the 33rd Structures, Structural Dynamics, and Materials Conference*, Dallas, Texas, April 13 – 15, 1992, pp. 514 – 524.

5. Reissner, E., 1972, "On Sandwich-Type Plates with Cores Capable of Supporting Moment Stresses," *Acta Mechanica*, Vol. 14, pp. 43 – 51.

6. Pagano, N. J., "Exact Solutions for Composite Laminates in Cylindrical Bending," *Journal of Composite Materials*, Vol. 3, No. 7, 1969, pp. 397 – 411.

7. Pagano, N. J., "Influence of Shear Coupling in Cylindrical Bending of Anisotropic Laminates," *Journal of Composite Materials*, Vol. 4, No. 7, 1970, pp. 330 – 343.

8. Jones, R. M., *Mechanics of Composite Materials*, McGraw Hill, New York, 1975, pp. 47 – 52.

9. Tessler, A., and Saether, E., "A Computationally Viable Higher-order Theory for Laminated Composite Plates," *International Journal for Numerical Methods in Engineering*, Vol. 31, pp. 1069 – 1086.

Undeformed State

Deformed State

$hw_i(x_1,x_2,x_3)\,\mathbf{B}_i(x_1,x_2)$

$\mathbf{b}_3$

$\mathbf{b}_2$

$\mathbf{b}_1$

$\mathbf{B}_3\,(x_1,x_2)$

$\mathbf{B}_2\,(x_1,x_2)$

$\mathbf{u}(x_1,x_2)$

$\mathbf{B}_1(x_1,x_2)$

$\hat{\mathbf{r}}(x_1,x_2,x_3)$

$\mathbf{r}(x_1,x_2)$

$\hat{\mathbf{R}}(x_1,x_2,x_3)$

$\mathbf{R}(x_1,x_2)$

O
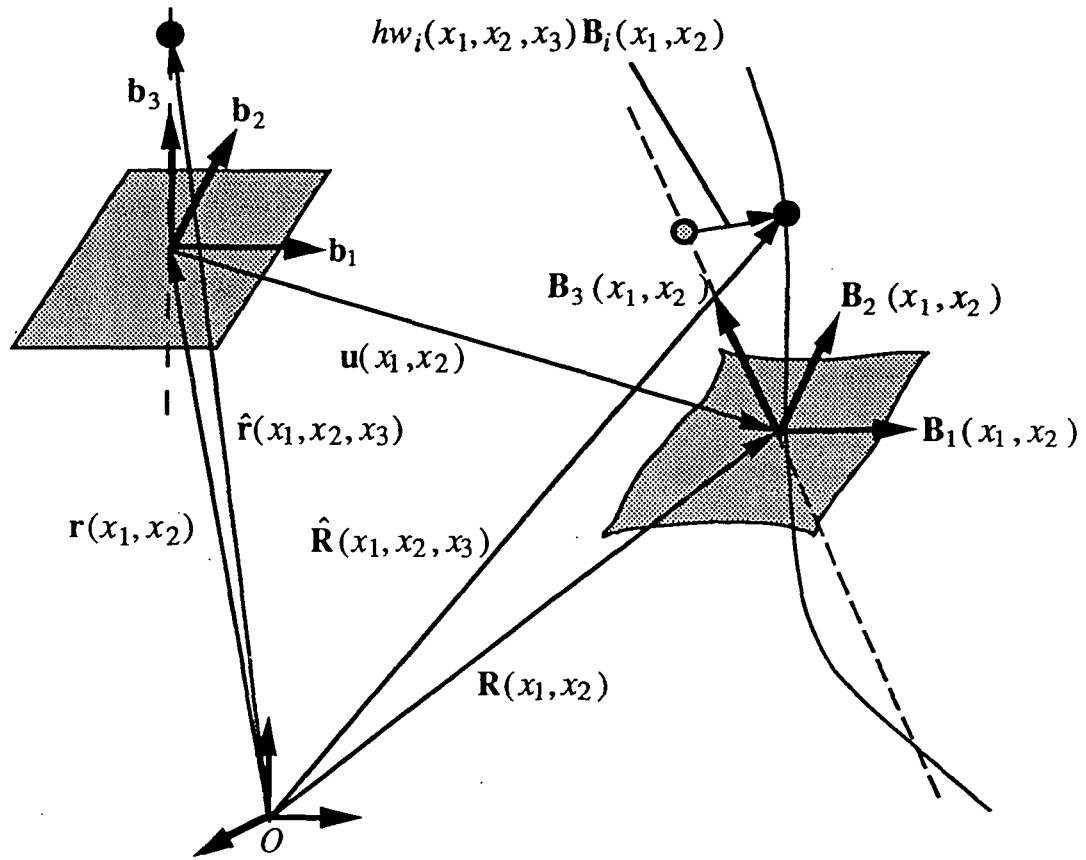
Fig. 1: Schematic of plate deformation

x_3

f_3

h

x_1

·L
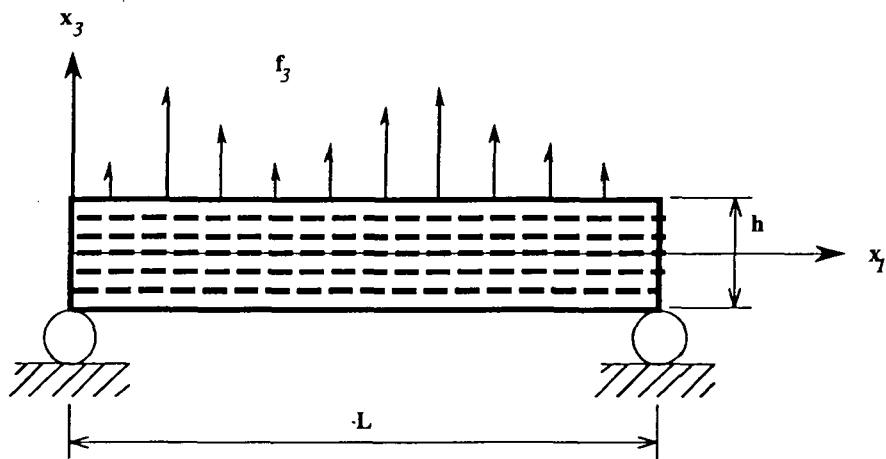
Fig. 2: Configuration of Cylindrical Bending of Plate
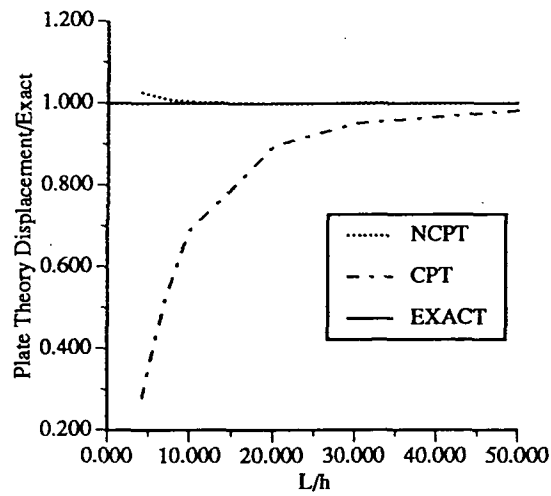
Fig. 3: Transverse Displacement for [15°] Plate
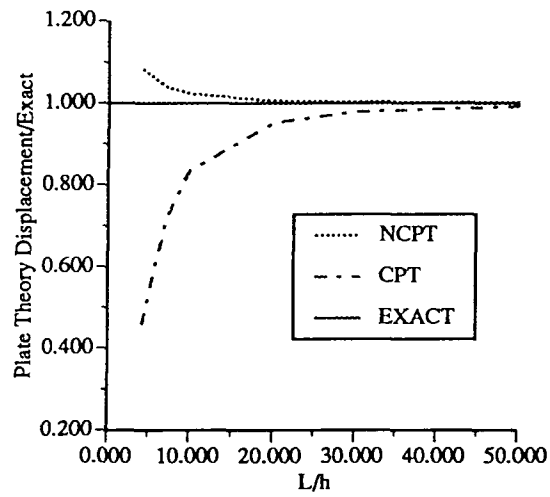
Fig. 4: Transverse Displacement for [15°/ − 15°] Plate
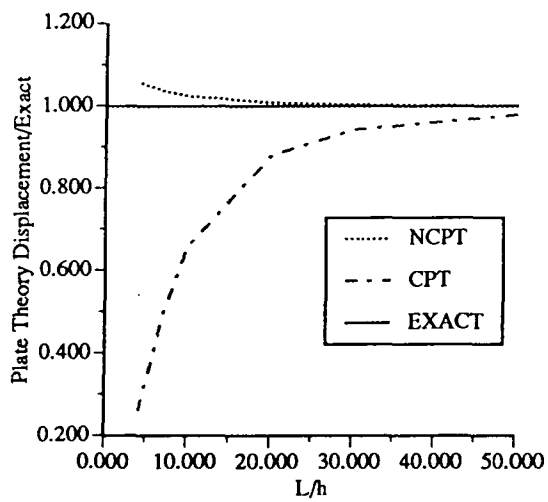
Fig. 5: Transverse Displacement for $[30°/ − 30°]_{sym}$ Plate
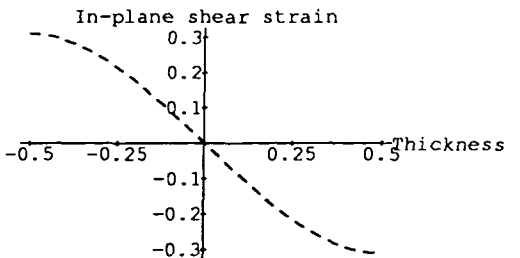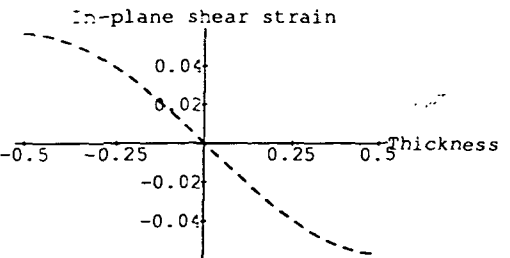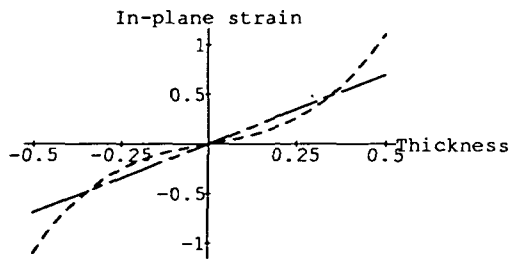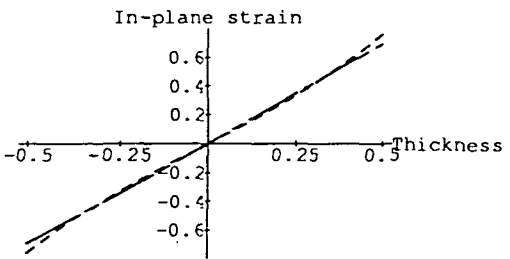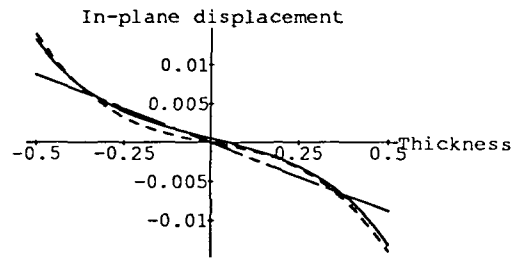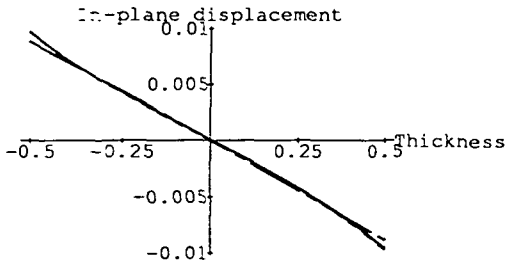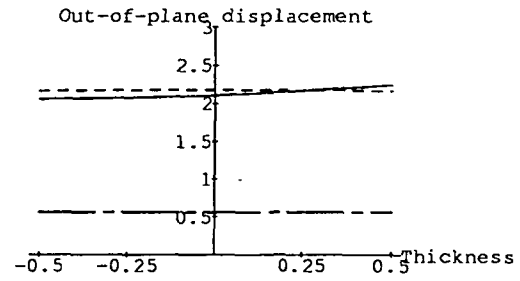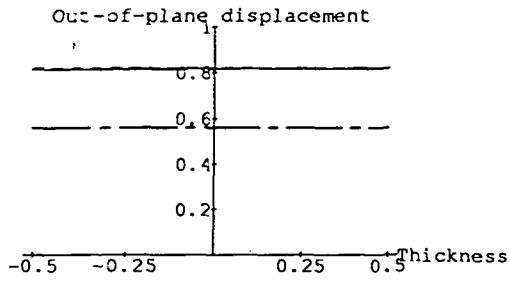
Fig. 6: Distributions of Normalized Quantities for [15°] Plate when $L/h = 10$

Fig. 7: Distributions of Normalized Quantities for [15°] Plate when $L/h = 4$
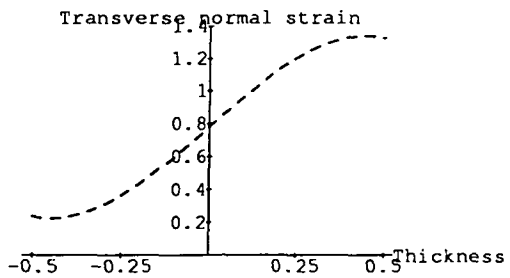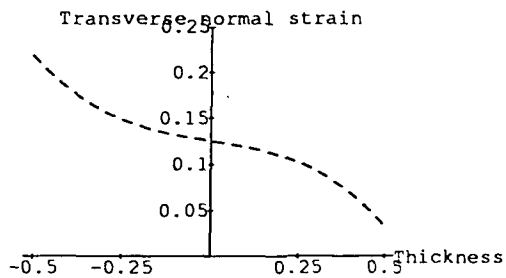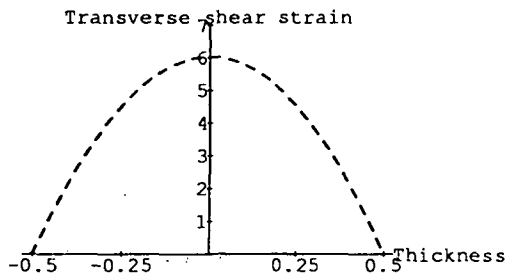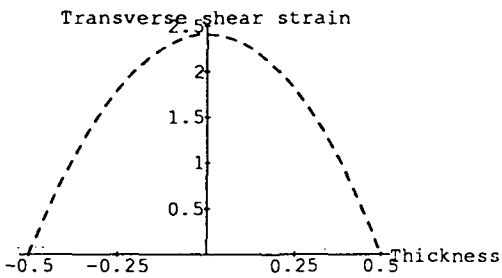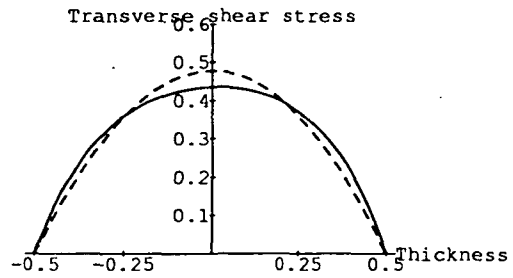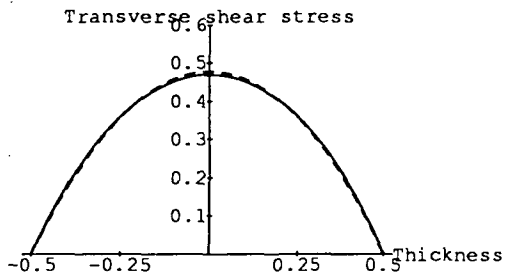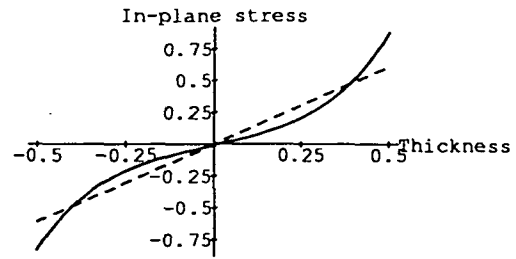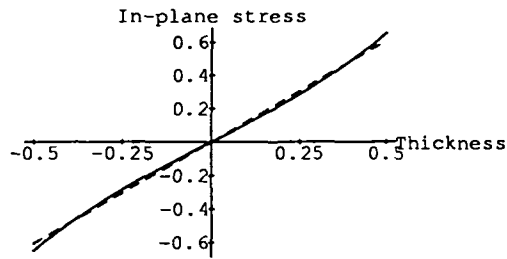
Fig. 8: Distributions of Normalized Quantities for [15°] Plate when $L/h = 10$

Fig. 9: Distributions of Normalized Quantities for [15°] Plate when $L/h = 4$
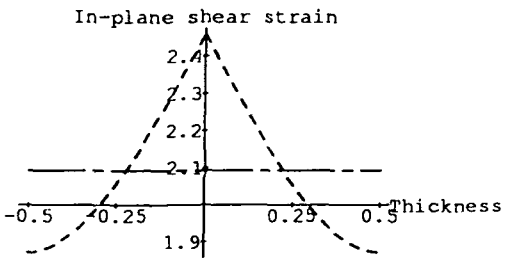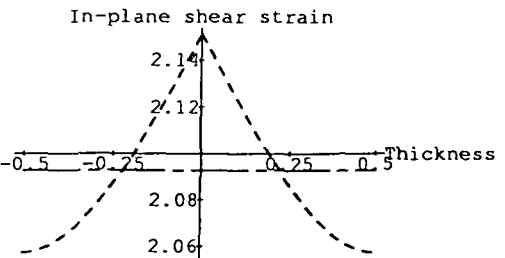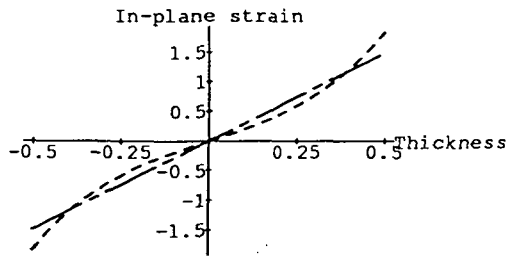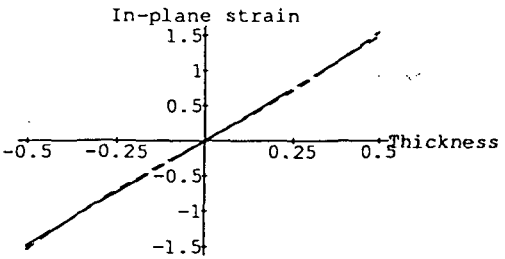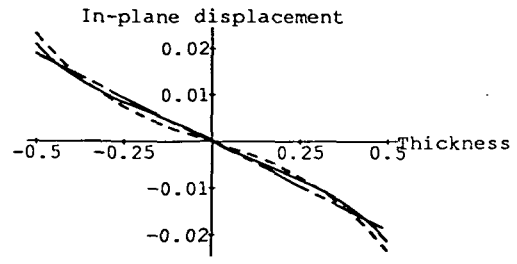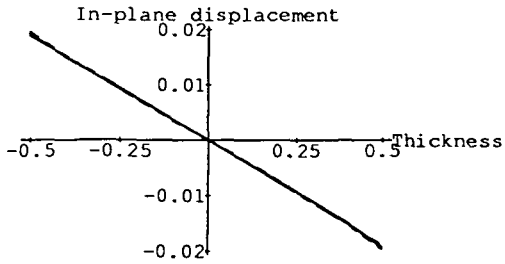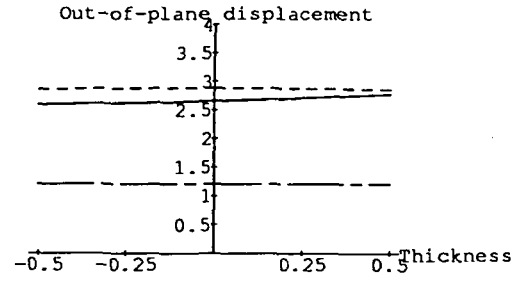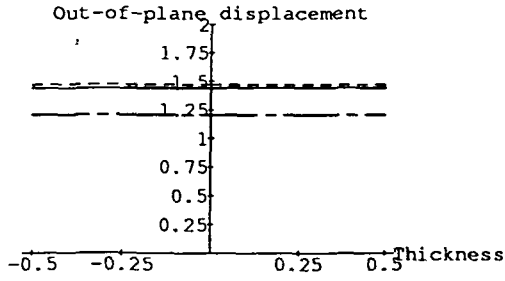
Fig. 10: Distributions of Normalized Quantities for [15°/ − 15°] Plate when $L/h = 10$

Fig. 11: Distributions of Normalized Quantities for [15°/ − 15°] Plate when $L/h = 4$

21
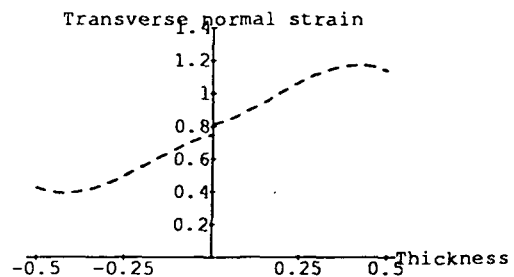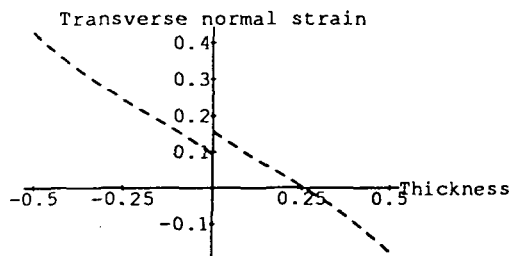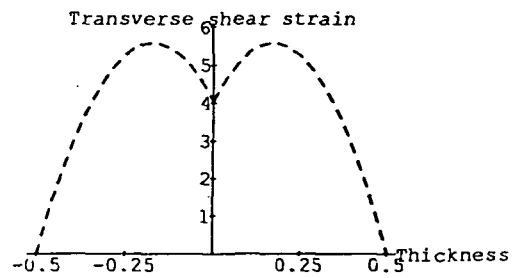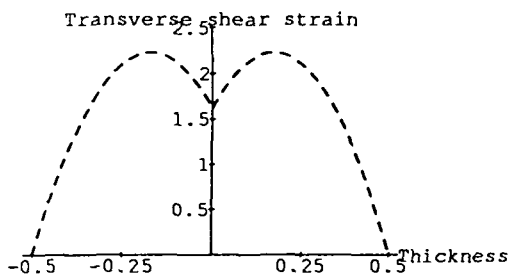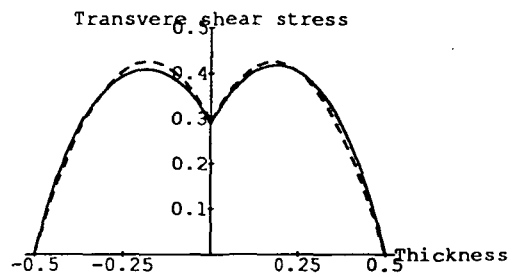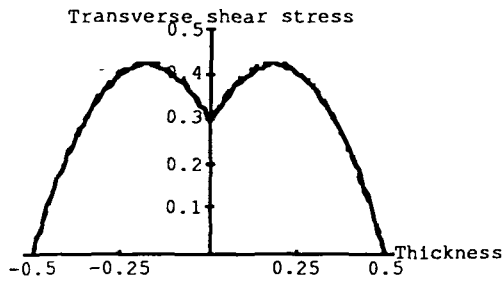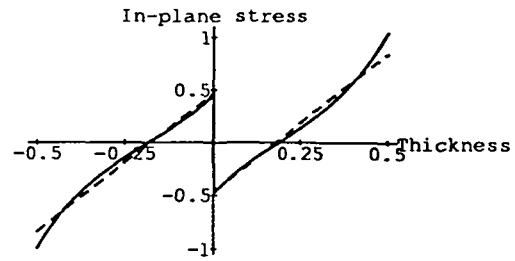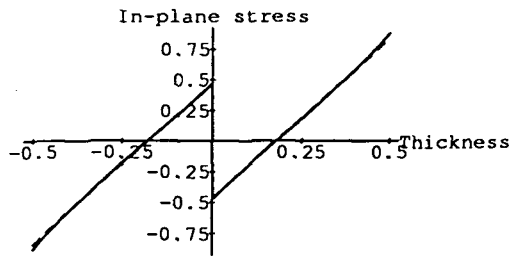
Fig. 12: Distributions of Normalized Quantities for [15°/ − 15°] Plate when $L/h = 10$

Fig. 13: Distributions of Normalized Quantities for [15°/ − 15°] Plate when $L/h = 4$

Out-of-plane displacement

In-plane displacement

Transverse in-plane displacement

In-plane strain

——— Exact; - - - - - - NCPT; —·—·— CLPT

Out-of-plane displacement

In-plane displacement

Transverse in-plane displacement

In-plane strain
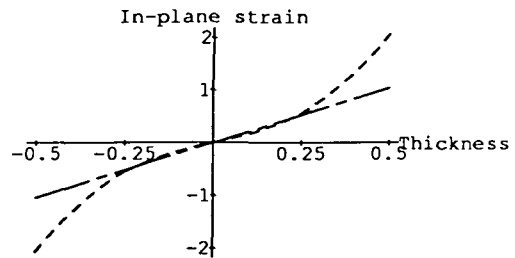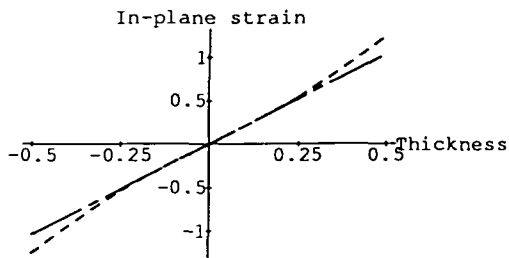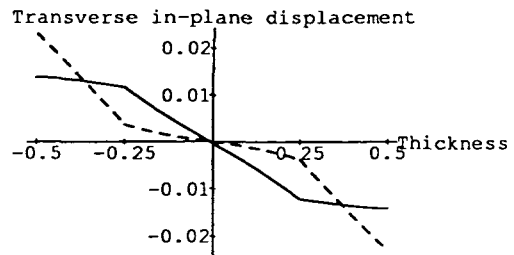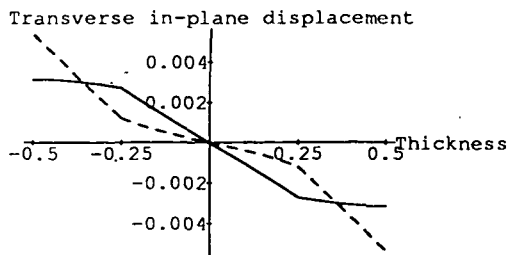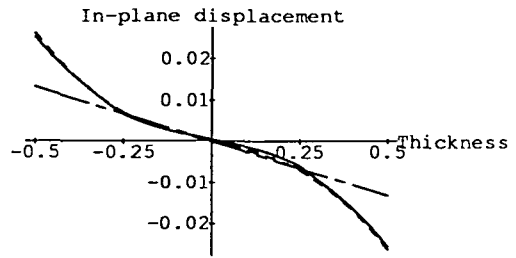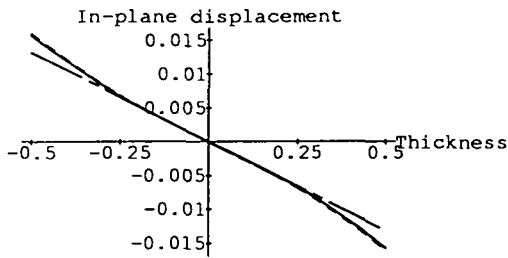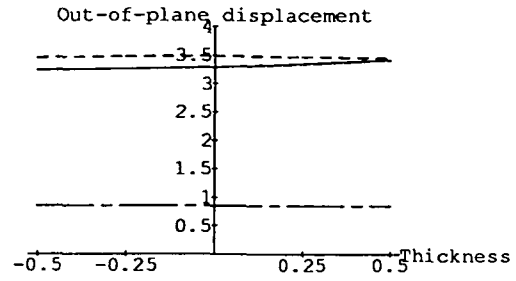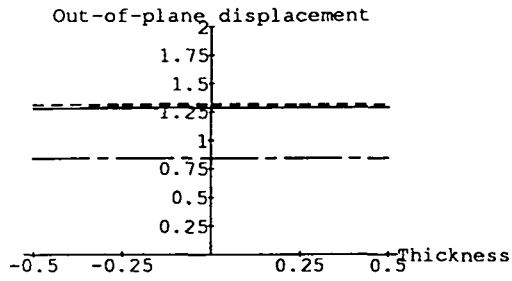
——— Exact; - - - - - - NCPT; —·—·— CLPT

Fig. 14: Distributions of Normalized Quantities for $[30°/-30°]_{sym}$ Plate when $L/h = 10$

Fig. 15: Distributions of Normalized Quantities for $[30°/-30°]_{sym}$ Plate when $L/h = 4$
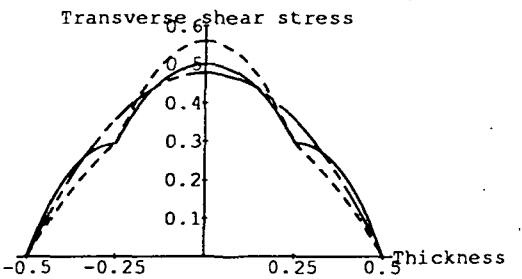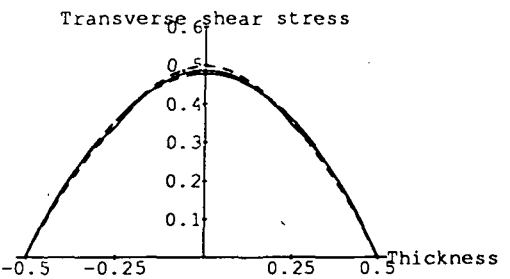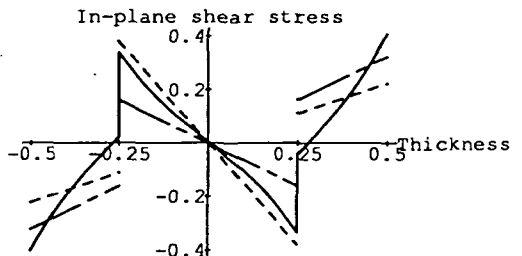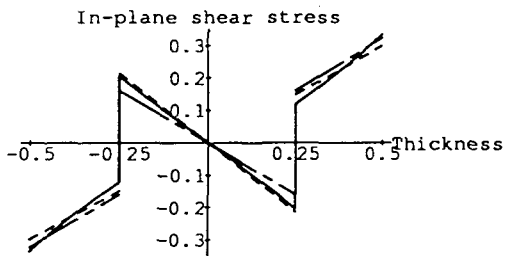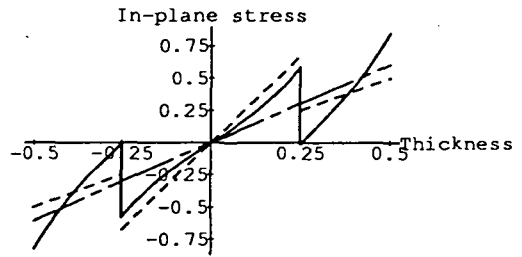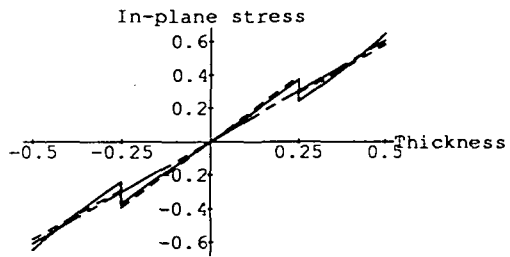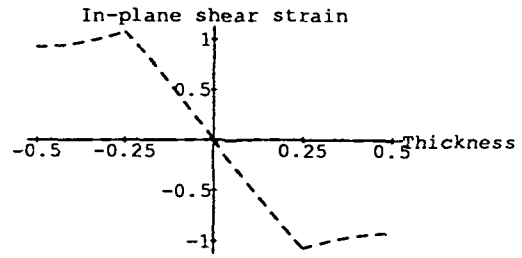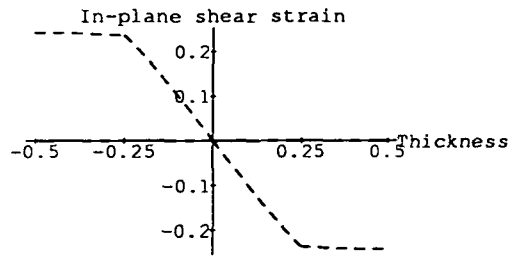
Fig. 16: Distributions of Normalized Quantities for $[30°/-30°]_{sym}$ Plate when $L/h = 10$

Fig. 17: Distributions of Normalized Quantities for $[30°/-30°]_{sym}$ Plate when $L/h = 4$
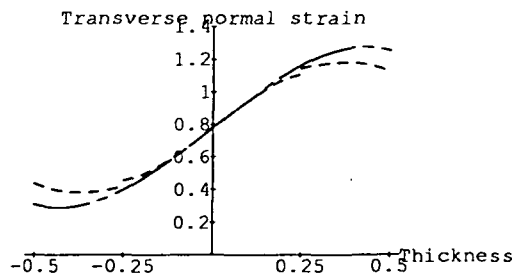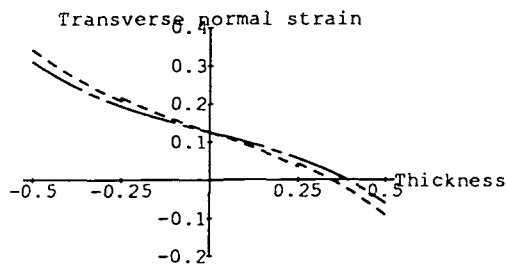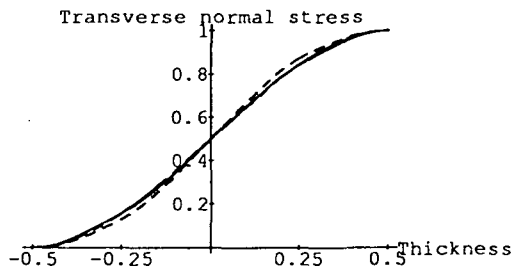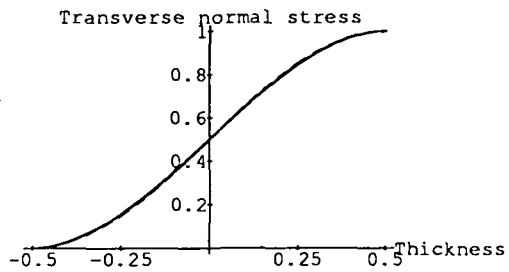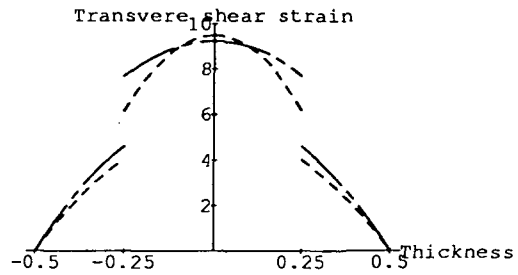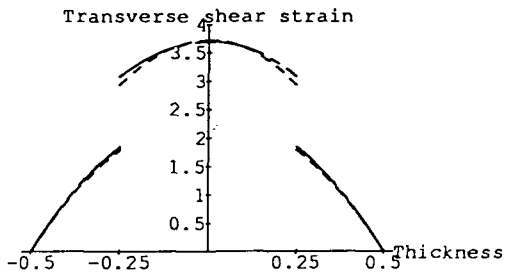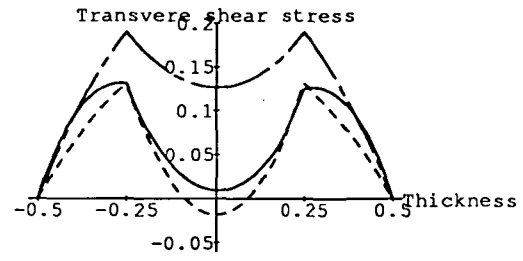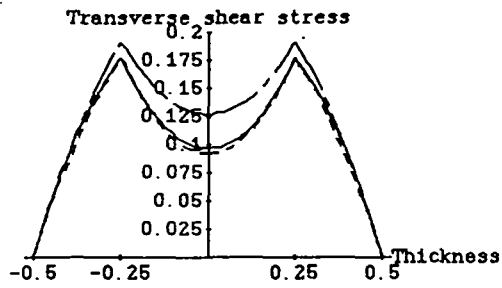
Fig. 18: Distributions of Normalized Quantities for $[30°/-30°]_{sym}$ Plate when $L/h = 10$

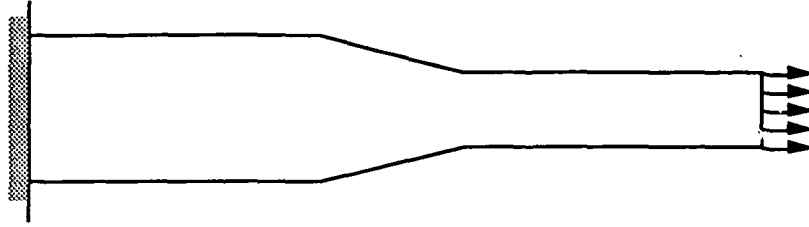Fig. 19: Distributions of Normalized Quantities for $[30°/-30°]_{sym}$ Plate when $L/h = 4$

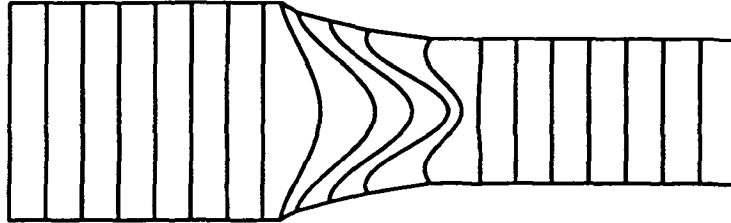Fig. 20: Tapered plate subjected to large in-plane force

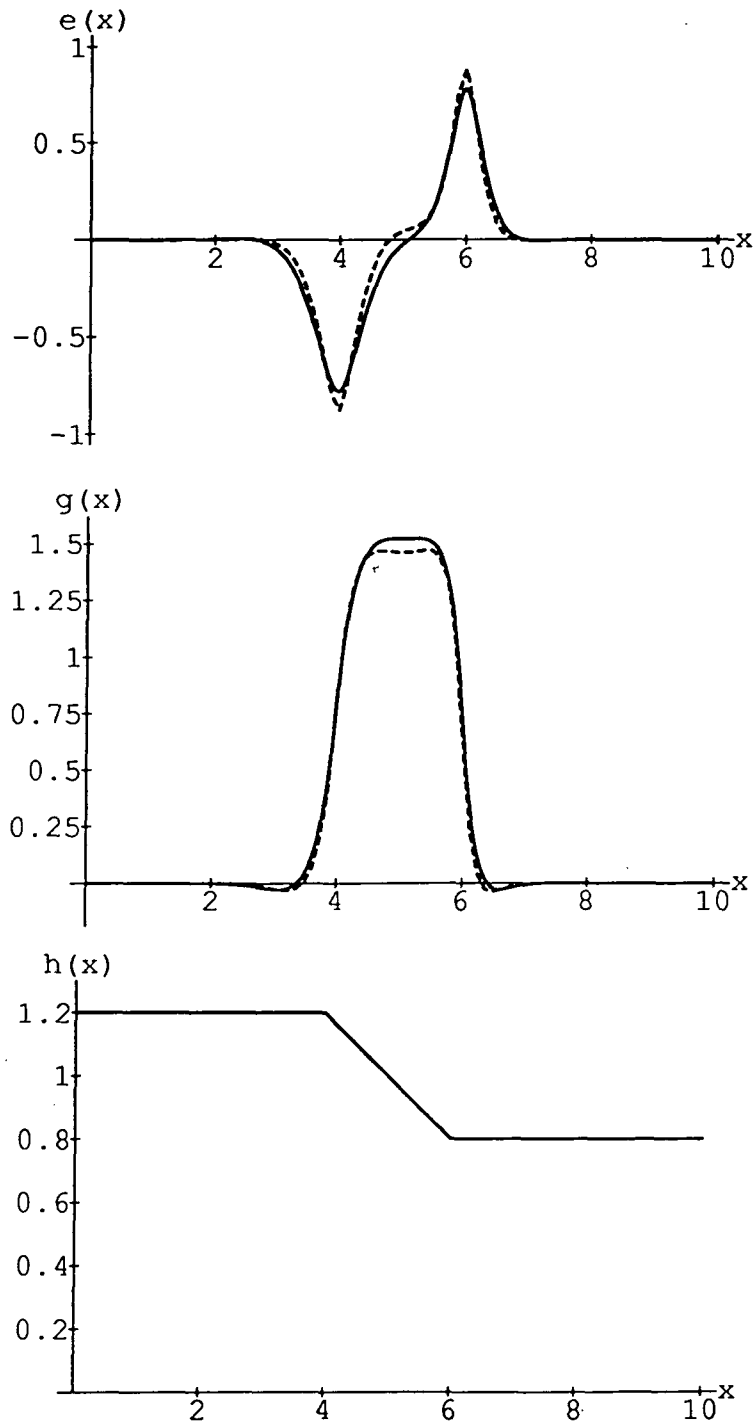Fig. 21: Exaggerated deformation of normal line elements for tapered plate

Fig. 22: Degrees of freedom from plate theory and three-dimensional results compared (solid lines are 3-D results and dashed lines are plate theory results)